[1]J. Shankar
[2]G. Mallesham
[3]Surrender Reddy Salkuti

Optimal Tuning of PI Controller for Automatic Generation Control in Multi-Area Power Systems Using PSO for Enhanced Load Frequency Control

Abstract: - This paper presents a novel approach for improving the load frequency performance in Multi Area Automatic Generation Control. The administration and regulation of certain components of a large hydrothermal power plant are challenged by the connectivity generated by wind power plants with varying ratings. Frequency transfers fall short when the generator's shaft speed falls below a predetermined threshold and the system frequency diverges from the intended value. Variations in the load demand are the source of this. In this work, a proportional-integral (PI) controller controls several parameters of an interconnected power plant. A PI controller ensures that such a power system runs as intended. The parameters of PI controllers are optimized using several readily available optimization techniques, such as Particle Swarm Optimization (PSO). Each algorithm uses a different cost function, like the square error multiplied by integral time, to evaluate the controller parameter (ITSE) and determine the most practical controller parameter choice. When several parameters need to be tuned at once, this trial-and-error process becomes quite time-consuming. A quicker and more effective method for optimizing various gains in load frequency management is the optimized-based approach or PSO. An integrated thermal, wind, and hydropower system created with MATLAB/Simulink has been simulated to evaluate the proposed model. Additionally, this study provides an overview of the effects of optimization strategy in the context of varying load scenarios.

Keywords: Proportional Integral (PI) Controller, Particle Swarm Optimization (PSO), Optimization Techniques, Load Frequency Control, and Automatic Generation Control (AGC)

INTRODUCTION

In modern times, the growing population and rising demand for electricity make conventional sources of energy inadequate to meet the growth. Thus, tie lines are required to establish a connection between various independent conventional sources in order to tackle this problem. The loads could be shared amongst the various sources and could withstand changes in the power system with ease because to their interconnectedness. The frequency of the system is impacted even though there is a greater chance of benefit from connecting between various places when there is load variation. If the load varies or changes for whatever reason while the single energy source is operating, only that energy source's frequency is impacted. However, when many energy sources are operating, all variations in load in any part of the power system affect not just the frequency but also the power delivered across the tie line. Because the main controller previously depended on the governor's action to restore the system's operating frequency to its pre-disturbance value, there is still a steady state frequency error. Consequently, an additional controller is employed, which raises the system's order while eradicating the steady-state error. This controller is referred to as a secondary or integrated controller. Because it delivers electricity in a more reliable and improved form, LFC is essential to the functioning and management of the power system.

Restoring the system tie line power and frequency to their baseline levels before the disruption is one of LFC's most significant responsibilities. Controlling the generating units' usable power will help achieve this [1-4]. Everyone is aware of the continual fluctuations in the load during the day. During a power system's steady-state operation, kinetic energy that is stored in the generator prime mover set modifies the load demand, resulting in a proportional shift in speed and frequency. A review and a state-of-the-art assessment of the AGC of power systems have been published in [5-6], respectively. There, several approaches to solving the AGC issue have been investigated. Thus, load frequency regulation is crucial to the electrical system's safe operation [7–11]. The most recent advancements in LFC techniques and methodology for various conventional and renewable energy-based power systems are thought to be found in the Automatic Generation Control (AGC).

[1]*Corresponding author: Research Scholar, Department of Electrical Engineering, University College of Engineering, OU, Hyderabad, Telangana, India
2 Professor, Department of Electrical Engineering, University College of Engineering, OU, Hyderabad, Telangana, India
3 Professor, Department of Railroad and Electrical Engineering, Woosong University, Daejeon 34606 Korea
*Corresponding author: shankar.jngm@gmail.com

It addresses both single- and multi-area power systems falling into these two groups. A power system ought to be regulated and restricted to a specific degree of deviation [12–17]. Better control strategies, including PID controllers combined with soft computing and optimization techniques, have been developed on automatic generation control (AGC) / load frequency control studies to increase transient responsiveness [18–22]. Control perspectives concerning frequency and power control have also been featured. The combined actions of unstructured and self-organized systems are known as swarm intelligence [23–25]. Swarm is made up of several separate agents, each with a finite amount of power. Numerous artificial algorithms that target optimization problems have been created based on intelligence of swarms [26–27].

I. THE COMPREHENSIVE THEORETICAL BASIS:

The Reheat thermal, wind, and hydroelectric components of the system have respective power outputs of 2000 MW, 35 MW, and 2000 MW. Through a tie line, these plants transfer power [28–29]. The Reheat thermal structure of the system was developed with consideration for the restrictions of both generating rate and reheat thermal [30–32]. It has long been assumed that wind farms are always in operation. There are three separate PI controllers in every system. For each of the three plants, transfer function models have been developed to do frequency response analysis. To minimize framework and analytic approaches, models are constructed using a linear approach [33]. A transfer function model for the wind power plant is created based on the assumption of a constant wind speed, and the wind power plant, which has a nominal rating of 35 MW, is further connected to the three Area Networks [34]. Figs. 4 and 5 depict the block diagram and pictorial representation of the connections between the three power systems. The list of various characteristics of a thermal-wind-hydropower system is displayed in Table 1. The three-area network is linked to a wind power facility with a nominal rating of 35 MW. The wind power system's transfer function model shows the hydro unit, the Wind Energy Conversion System (WECS), the generic speed governing system model, and the wind power plant constructed under the assumption of constant wind speed.

A. Thermal Power Station:

The highly pressurized steam in a thermal power plant is used to recover thermal potential energy, which is then used to power a generator. The first unit in the Simulink model in Fig. 1 is the governor, which regulates the quantity of steam that enters the turbine. The following is a representation of a governor's transfer function:

$$G_{gt}(s) = \frac{K_g}{T_g.s + 1} \tag{1}$$

The turbine expands with the pressurized steam that enters through a steam inlet valve. The transfer function of the steam turbine can be represented as follows:

$$G_{Tt}(s) = \frac{K_t}{T_t.s + 1} \tag{2}$$

The Steam exhaustion and an increase in moisture content are caused by the expansion of steam inside a turbine. Consequently, in order to remove any remaining moisture, the steam produced by the steam turbine needs to be heated again. A common approach to express the transfer function of a conventional re-heater is as

$$G_{Rh}(s) = \frac{K_r.T_r.s + 1}{T_r.s + 1} \tag{3}$$

The turbine is mechanically coupled to an electric generator. Such a generator's transfer function can be expressed as follows:

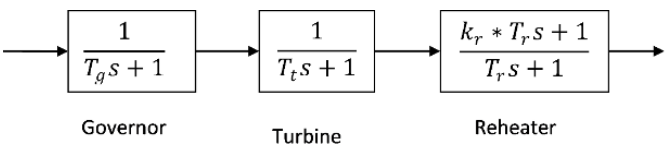

Fig.1 Mathematical Modeling of Reheat Thermal Power station

B. Hydro Power Station:

Water is kept in hydroelectric power plants to a height known as the "head." When the dammed water is forced to flow downward via the penstock and into the turbine, its potential energy is transformed into kinetic energy, which powers the turbine to produce electricity. The hydro governor is the initial block in the Simulink model of a hydroelectric power plant of Fig.2. A hydroelectric plant governor's transfer role can be expressed as follows:

The hydraulic turbine's transfer function is

$$G_{Ht}(s) = \frac{-T_{wt}.s + 1}{0.5T_{wt}.s + 1} \tag{4}$$

Transfer function of hydraulic Governor is,

$$\frac{K_d.s^2 + K_p.s + K_i}{K_d.s^2 + \left(K_p + \frac{f}{R_2}\right)s + K_i} \tag{5}$$

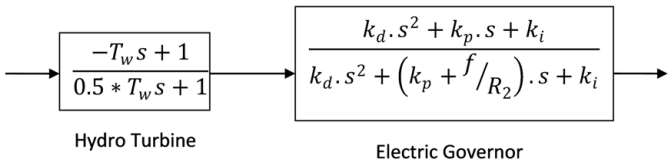

Fig.2 Mathematical Modeling of Hydro Power station

C. Wind Energy Conversion System:

The two-pole-one-zero transfer function illustrated below can be used to explain the dynamic operation of the Wind Energy Conversion System (WECS): Wind Energy Conversion System (WECS) natural frequencies and damping ratios are determined by the poles of the transfer function, where Tϵ and Tpt are the parasitic and main time constants, respectively. It adds new dynamics, like oscillations, settling time, and overshoot, that might affect how the system behaves. The mathematical model block in Fig. 3's Simulink model that represents a wind turbine plant is the WECS.

By choosing the suitable natural frequency ω_n and damping factor γ, the wind energy conversion system's second-order dynamics may be obtained, which in turn provides the controller settings.

$$T_i = \frac{2\gamma}{\omega_n} - \frac{1}{\omega_n^2 T_{pt}} \tag{6}$$

$$K_p = \left(\frac{T_i T_p}{K_{pt}}\right)\omega_n^2 \tag{7}$$

$$H_{pt}(s) = \frac{K_{pt}(T_{zs} + 1)}{(T_{\varepsilon s} + 1)(T_{pt} + 1)} \tag{8}$$

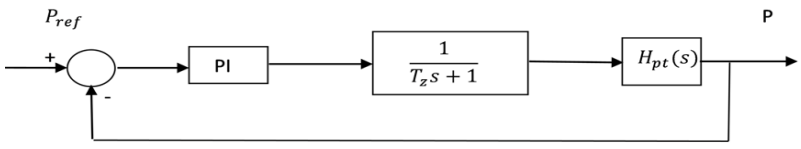

Fig.3 Mathematical Modeling of WECS

The Integral Time Square Error (ITSE) was chosen as the performance index, which can be written as:

$$ITSE = \int \left\{ (\Delta f_i)^2 + \left(\Delta P_{tie_{i-j}} \right)^2 \right\} t.dt. \quad (9)$$

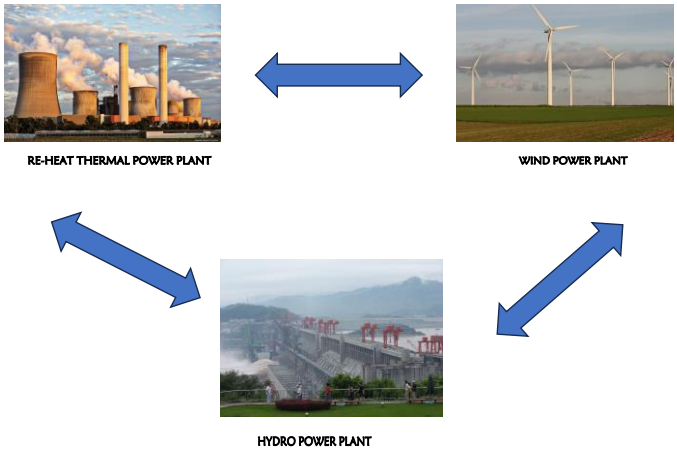

Fig.4 A graphical representation of three distinct yet linked regions via a tie-line

Table:1 Parameters of Simulated System

Parametric Specifications of the Simulated Reheat Thermal and Hydro Power Plant	
P_r	2000Mw
K_r	0.5
T_g	0.08sec
T_t	0.3sec
f	50Hz
K_p	120Hz/p. u Mw
T_r	10sec
$P_{tie\ max}$	200Mw
T_p	20sec
H	5 sec
P_r	35 Mw
D	0.00833 p.u. Mw/Hz
R	2.4 Hz/p.u. Mw
Parametric Wind Power Plant Simulation Specifications	
Density of Air	1.2 kg/m^3
Gear ratio	70
T_{pt}	10.55
Radius of turbine blade	45m
K_{pt}	0.012
H	5 sec
Average wind velocity	7m/s
T_i	3 sec
T_p	20 sec
T_{12}	0.544

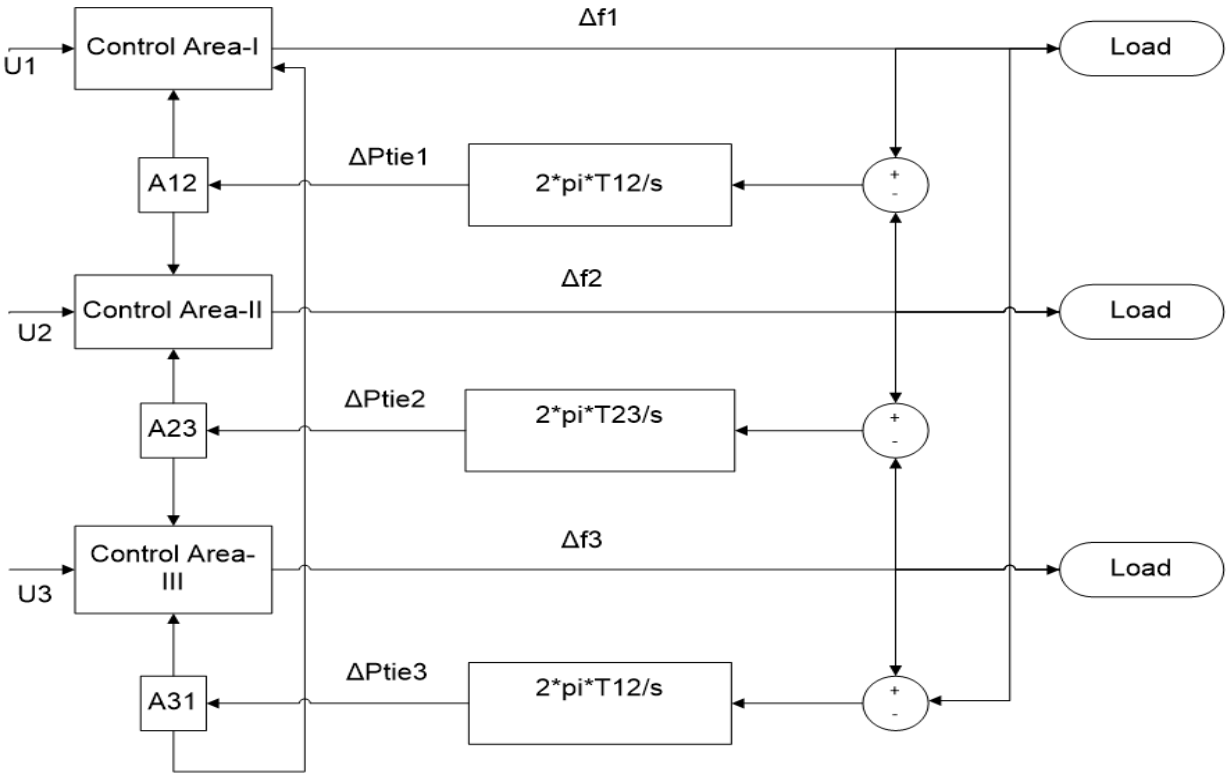

Fig.5 Block schematic Illustration of a three-area system which is interconnected

II. CONTROL METHODOLOGY

A. Proportional Inegral (PI) Controller

Through the mitigation of the individual's disadvantages, the PI controller is utilized, which combines the benefits of the integral and proportional controllers. Equation (10) provides the conventional PI controller's transfer function, where Kp and Ki stand for the controller's parameters.

$$H(s) = \frac{U(s)}{E(s)} = K_p + {K_i}/{s} \tag{10}$$

Equation (11) also illustrates the PI controller's time domain representation. where the error-caused response, u(t), is given by e(t).

$$U(t) = K_p + K_i \int e(t)dt \tag{11}$$

B. PARTICLE SWARM OPTIMIZATION ALGORITHM (PSO)

Particle swarm optimization uses an initial population of individuals to search for optima, much like other evolutionary computation techniques. Then, using some sort of procedure, the members of this original population are updated and transferred to an improved area. Inspired by evolutionary phenomena observed in nature, four well-known evolutionary algorithms—genetically, evolutionary programming, genetic algorithms, and genetic algorithms. From there, they appropriate the ideas regarding competition and the evolution of the fittest. PSO, however, derives its motivation from social behavior simulation. It takes inspiration from the idea of individual rivalry and cooperation.

However, there are some ways in which this method is superior to genetic and evolutionary algorithms. PSO has memory first. In other words, each particle retains memory for the collective optimal solution (global best) and its optimal solution (local best). PSO also has the benefit of maintaining its initial population, eliminating the need to apply operators to the population. This procedure requires considerable amounts of time and memory storage. The PSO employs a stochastic search method improved by swarm intelligence to obtain findings in Table 2. PSO functions as an algorithm that utilizes collective intelligence as a result. This attempt includes a variety of randomly generated alternative solutions. Each of these possible fixes is referred to as a particle, and together they are called a swarm.

Every individual in the PSO system modifies their flying in a multi-dimensional search space based on their own and their companions' flying experiences. Every person is called a "particle," which stands for a potential fix for the issue. When the number of iterations increases by one, the coordinates of location (x) and velocity (v) align. Every particle in a D-dimensional space is regarded as a point. The ith particle is represented as X_i^k is ($x_{i1}^k\ x_{i2}^k\ x_{i3}^k \dots\dots\dots x_{iD}^k$)T For a particle, the rate of position change (velocity) g is expressed as V_i^k is ($v_{i1}^k\ v_{i2}^k\ v_{i3}^k \dots\dots\dots v_{iD}^k$)T indicates its current movement decision. Any particle's best prior location, which provides the highest fitness value, is noted and shown as P_i^k ($p_{i1}^k\ p_{i2}^k\ p_{i3}^k \dots\dots\dots p_{iD}^k$)T is Among all the particles in the population, the best particle's index is shown. Equation (12) describes a velocity update equation that modifies the i th particle's velocity.

Table:2 PSO Simulation Parameters

PSO Parameters	
Swarm size	100
Problem dimension	6
Number of iterations	50
PSO coefficient of acceleration c1	2
PSO coefficient of acceleration c1	2
PSO Inertia's weight: w_{max}	0.9
PSO Inertia's weight: w_{min}	0.4

B.1 Equation for updating velocity

The velocity update equation is used in Particle Swarm Optimization (PSO) to adjust the velocity of each particle in the swarm, refreshing their positions in the search space. To balance exploration and exploitation during the optimization process, this equation combines cognitive and social components. The following is the typical velocity update equation:

$$V_i^{k+1} = wv_{iD}^k + c_1 * r_1\left(P_{iD}^k - X_{iD}^k\right) + c_2 * r_2\left(P_{gD}^k - X_{iD}^k\right) \quad (12)$$

B.2 Equation for Position Update

The position update equation is used in Particle Swarm Optimization (PSO) to modify each particle's position in the swarm according to its updated velocity.

$$V_{iD}^{k+1} = X_{iD}^k + V_{iD}^{k+1} \quad (13)$$

While i is 1, 2……. indicates the particle index, D is 1, 2……..., which stands for dimensions. The acceleration constants for the social and cognitive scaling features are C1 and C2, respectively, while the swarm size is represented by the letter S. Integers between zero and one are uniformly dispersed at random over both r1 and r2.

Each particle's dimensions are updated independently, as demonstrated by (12) and (13). Only the best-found gbest and pbest are connected to the issue space dimensions by the goal function. The PSO algorithm is defined by algebras (12) and (13). The PSO approach procedure in the flow chart algorithm is depicted in Fig. 2.

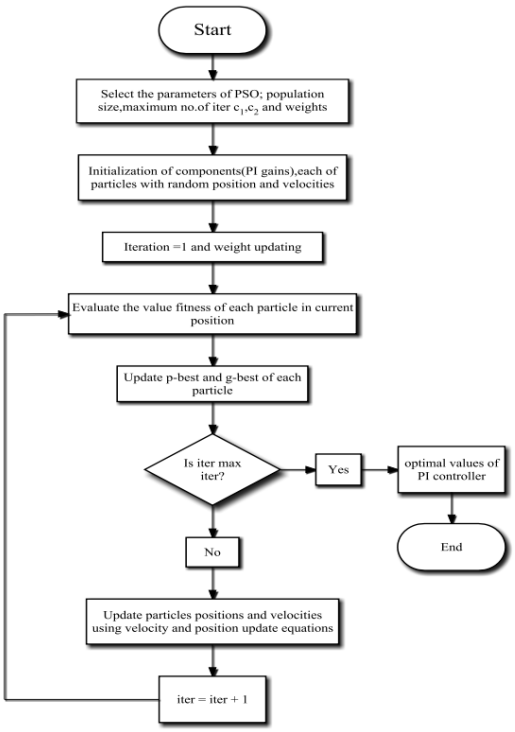

Fig.6 Flowchart of PSO Algorithm

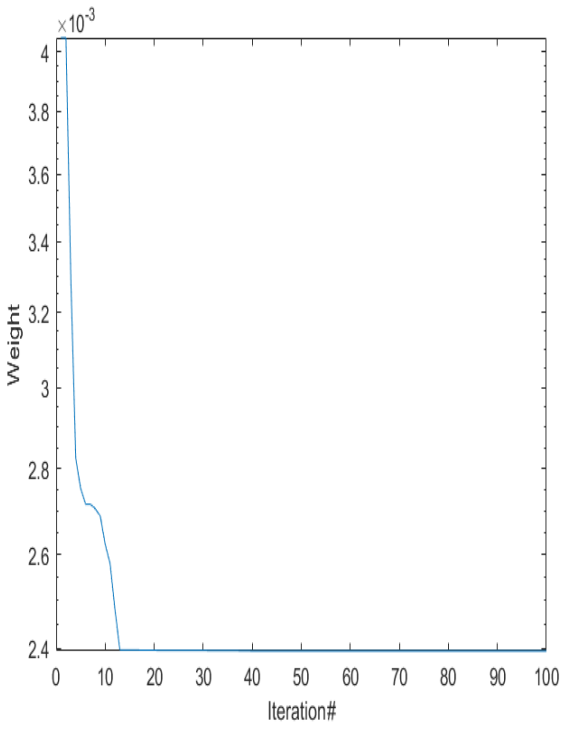

Fig.7 PSO Cost function

III. RESULTS AND DISCUSSION

After the text edit has been completed, the paper is ready for the template. Duplicate the template file by using the Save As command, and use the naming convention prescribed by your conference for the name of your paper. In this newly created file, highlight all of the contents and import your prepared text file. You are now ready to style your paper. The optimization issues, PI Controllers, and load frequency regulation received a lot of attention. It is well known that the power system maintains system parameters within permissible bounds and can sustain its load while operating normally. On the other side, the system variables are impacted by an abrupt breakdown in the power system. Controllers must be utilized to overcome this issue. The principal control loop of a power system is considered an extra controller. Utilizing the error signal from the power system, the PI controller which functions as a secondary controller in the current study calculates the proper control signal to generate.

The power system uses the control signal that the controller generates as a reference signal. The system frequency and tie-line power flow error-connected associated regions are combined linearly to form the error signal. Thus, a multi-area reheat power system was planned and implemented using the MATLAB/Simulink environment, and it was examined in this work. To assess the superior performance of the suggested method, a PI controller and step load perturbations (SLPs) of 1%, 2%, and 5% in Area 1 are employed to simulate the necessary power system. An independent MATLAB file contains the optimization algorithm that is developed and used to modify the controller's parameters. In this simulated scenario, the PSO method is considered for optimizing the gain values of the controller parameters.

A. 1% Step Load Disturbance in Area-1

In this Scenario The recommended controllers are applied to a 0.01 percent increase in load demand across the three regions in MATLAB/Simulink to mimic the recommended model. Figures 6 and 7 depict, respectively, the frequency variations, Tie-line power variations, and Area Control Error fluctuations of the Reheat thermal area, wind area, and hydropower area for the system dynamic reactions. The PSO-tuned controller has a quicker settling time than the conventional PI controller, but it has better peak overshoots and peak undershoots. In the end, the developed controller outperforms the other controllers in terms of dynamic responsiveness. With these factors and dynamic reactions in mind, the power transfer deviation via the tie line, frequency offset, and Area Control Error were computed at each of the three locations. As a result, for the closed-loop system, the observed system responses, tie-line power flow, and area control errors are displayed in Figs. 6 and 7. The suggested PSO-PI Controller has a substantially shorter settling time and overshoots than the traditional PI controller.

Figures 6 and 7 for the frequency variations, tie-line power, and area control error all clearly show this. It is clear that, in comparison to the other areas, area-1's frequency deviation has the largest undershoot peak. In contrast to the other areas, it has the least amount of overshoot peak. When compared to the other areas of the values, area-1 exhibits a positive overshoot peak in relation to the tie-line power flow. As a result, the recommended PSO-PI controller outperforms the conventional PI Controller for the Multi Area Power System. Summary of the controllers' gains is shown in table 3.

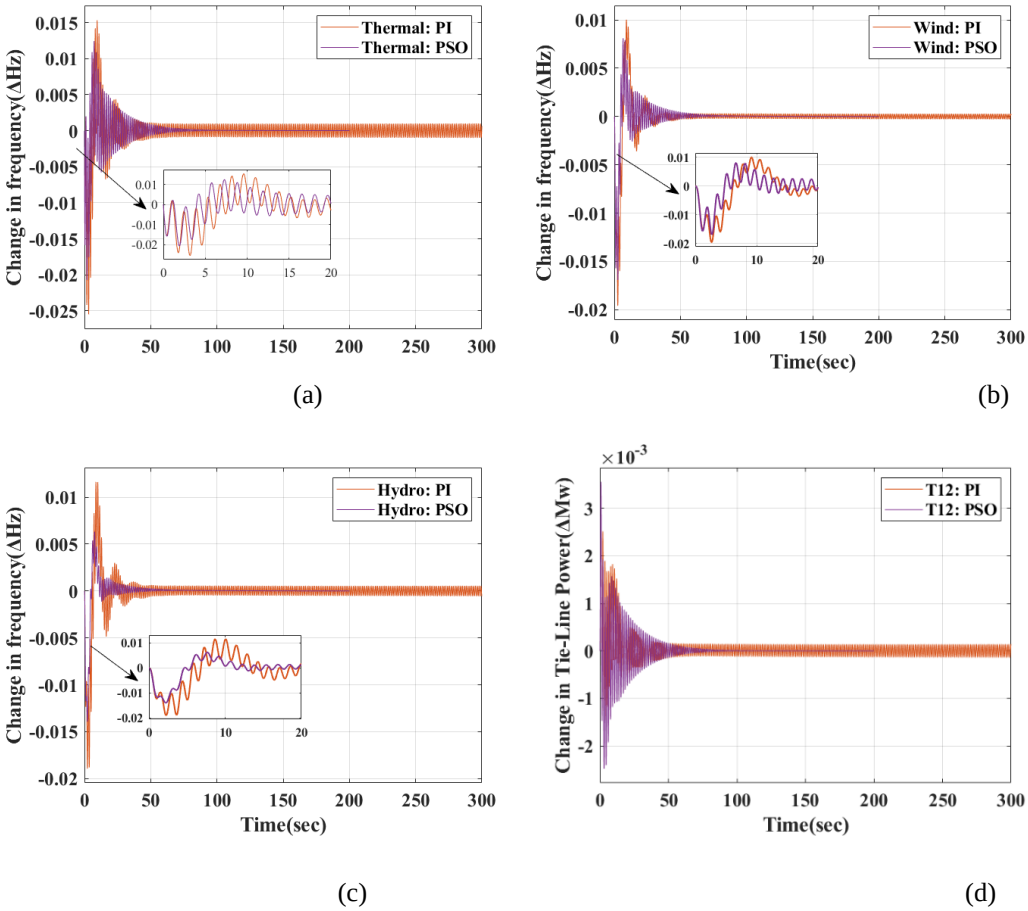

Figure 6: Evaluation of 1% Change in load in AREA-1; (a) Variations in Area-1 frequency, (b) Variations in Area-2 frequency, (c) Variations in Area-3 frequency, and (d) Variations in Area-1 and Area-2 Tie-Line Power

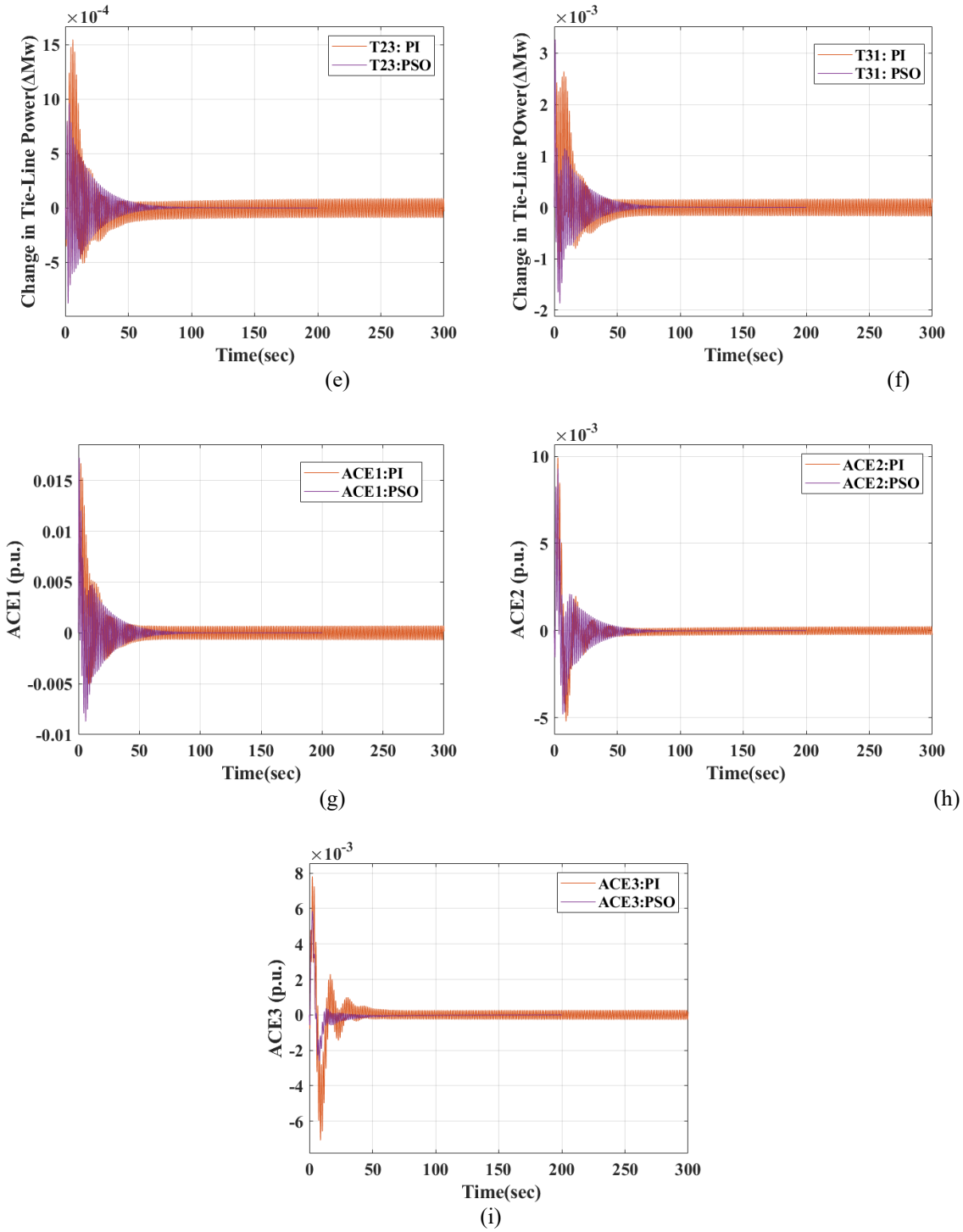

Fig.7. The attainment of a 1% Change in load in AREA-1; (e) Variation in Area-2 and Area-3 Tie-Line Power (f)
Variation in the Tie-Line Power between Areas 1 and 3. Area Control Errors for Areas 1 through 3 are shown in (g), (h), and (i) respectively.

Table:3 Steady State Error, Peak Under Shoot, Peak Over Shoot, and Settling Time Comparison Values for 1% Variation Load in Area-1

	STEADY STATE ERROR		PEAK OVER SHOOT		PEAK UNDER SHOOT		SETTLING TIME	
	PI	**PSO**	PI	**PSO**	PI	**PSO**	PI	**PSO**

ΔF_1	0.0006213	**-0.000003109**	0.01533	**0.01243**	-0.025451	**-0.020615**	oscillate	**90**
ΔF_2	0.0001396	**-0.000002738**	0.01002	**0.008106**	-0.019499	**-0.016926**	oscillate	**90**
ΔF_3	-0.0005511	**-0.00000872**	0.01164	**0.006330**	-0.018973	**-0.013968**	oscillate	**100**
ΔP_{tie1}	0.0006213	**-0.000003109**	**0.003364**	0.003556	**-0.0014492**	-0.002446	oscillate	**120**
ΔP_{tie2}	0.0001396	**-0.000002738**	0.001546	**0.000962**	**-0.0007691**	-0.0008446	oscillate	**120**
ΔP_{tie3}	-0.0005511	**-0.00000872**	**0.003100**	0.003265	**-0.0012029**	-0.001864	oscillate	**100**
ACE_1	0.0006213	**-0.000003109**	**0.01668**	0.02478	**-0.0050127**	0.0073276	oscillate	**100**
ACE_2	0.0001396	**-0.000002738**	0.009926	**0.009297**	-0.0052024	**-0.0047956**	oscillate	**100**
ACE_3	-0.0005511	**-0.00000872**	0.007814	**0.005846**	-0.0071068	**-0.0025824**	oscillate	**120**

B. 2% Step Load Disturbance in Area-1

In this Situation To observe the robustness of the system, the given model is simulated in MATLAB/Simulink with the suggested controllers applied to a 0.02 percent increase in load demand across the three areas. Figs. 8 and 9 show the frequency deviations, Tie-line power flow, and Area Control Error for the Reheat thermal zone, wind area, and hydro region, respectively, which reflect the system dynamic responses. The PSO-PI Controller has better peak overshoots and peak undershoots as well as steady state even though it settles faster than the PI controller. Table 4 displays the frequency deviation, tie-line power deviations, and area control error for the wind, hydro, and reheat thermal zones, respectively, as indicators of the system dynamic reactions. The PSO-PI Controller outperforms the PI Controller in terms of steady state error, peak overshoots, and peak undershoots, even though it settles faster. In terms of dynamic reactivity, the designed controller finally performs better than the other controllers.

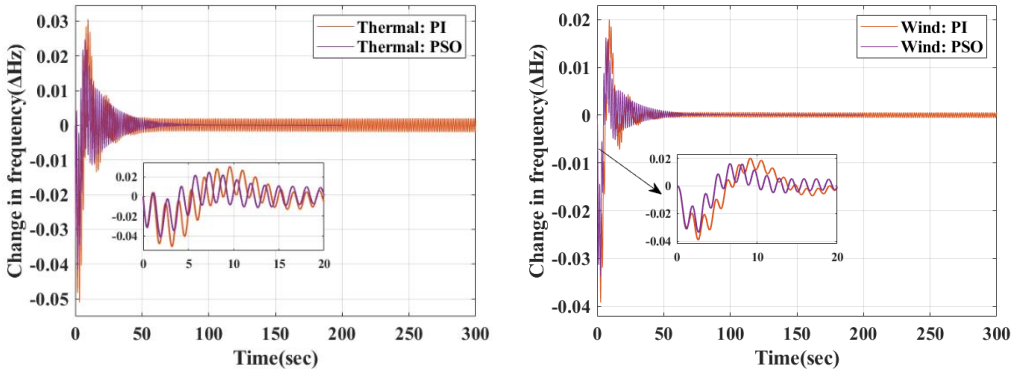

(a) (b)

Fig. 8. Evaluation of 2% Change in load in AREA-; (a) Variations in Area-1 frequency, (b) Variations in Area-2 frequency,

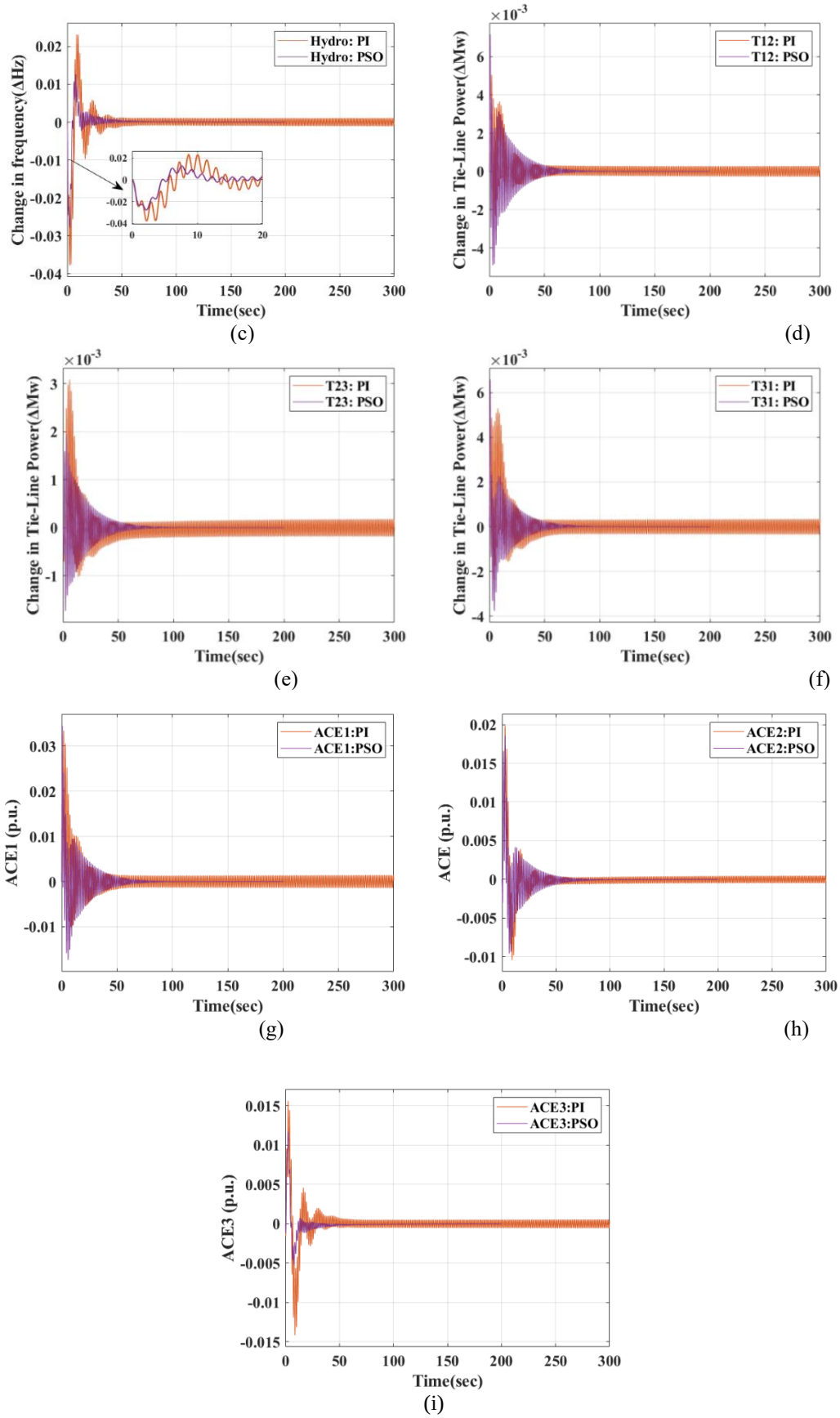

Fig.9. The attainment of a 2% Change in load in AREA-1; (c) Variations in Area-3 frequency, and (d) Variations in

Area-1 and Area-2 Tie-Line Power (e) Tie-line power change between Area-2 and Area-3 (f) Tie-line power change between Area-3 and Area-1; Area Control Errors for Areas 1 through 3 are shown in (g), (h), and (i) respectively.

Table:4 Comparison values of Steady State Error, Peak Over Shoot, Peak Under Shoot and Settling Time for 2% Change Load in Area-1

	STEADY STATE ERROR		PEAK OVER SHOOT		PEAK UNDER SHOOT		SETTLING TIME	
	PI	**PSO**	**PI**	**PSO**	**PI**	**PSO**	**PI**	**PSO**
ΔF_1	0.001277	**-0.000006219**	0.03051	**0.02471**	-0.0511	**-0.041355**	oscillate	**90**
ΔF_2	0.0002779	**-0.00005476**	0.02006	**0.01629**	-0.039221	**-0.033703**	oscillate	**90**
ΔF_3	-0.001118	**-0.00005744**	0.02316	**0.01266**	-0.037869	**-0.028049**	oscillate	**100**
ΔP_{tie1}	0.001277	**-0.000006219**	**0.006693**	0.007156	**-0.0029186**	-0.0049163	oscillate	**120**
ΔP_{tie2}	0.0002779	**-0.00005476**	0.003085	**0.001933**	**-0.0015401**	-0.0041324	oscillate	**120**
ΔP_{tie3}	-0.001118	**-0.00005744**	**0.006221**	0.006577	**-0.0023506**	-0.0037648	oscillate	**100**
ACE_1	0.001277	**-0.000006219**	**0.03340**	0.03450	**-0.010006**	-0.017231	oscillate	**100**
ACE_2	0.0002779	**-0.00005476**	0.01985	**0.01855**	-0.010433	**-0.009611**	oscillate	**100**
ACE_3	-0.001118	**-0.00005744**	0.01563	**0.01171**	-0.014126	**-0.0051811**	oscillate	**120**

C. 5% Step Load Disturbance in Area-1

In this case, to observe the robustness of the system, the given model is simulated in MATLAB/Simulink with the suggested controllers applied to a 0.02 percent increase in load demand across the three areas. Figs. 10 and 11 show the frequency deviations, Tie-line power flow, and region Control Error for the Reheat thermal zone, wind region, and hydro area, respectively, which reflect the system's dynamic responses. The PSO-PI Controller has better peak overshoots and peak undershoots as well as a steady state, even though it settles faster than the PI controller. Table 5 displays the frequency deviation, tie-line power deviations, and area control error for the wind, hydro, and reheat thermal zones, respectively, as indicators of the system's dynamic reactions. The PSO-PI Controller outperforms the PI Controller in terms of steady-state error, peak overshoots and undershoots, and settling time. In terms of dynamic reactivity, the designed controller finally performs better than the other controllers.

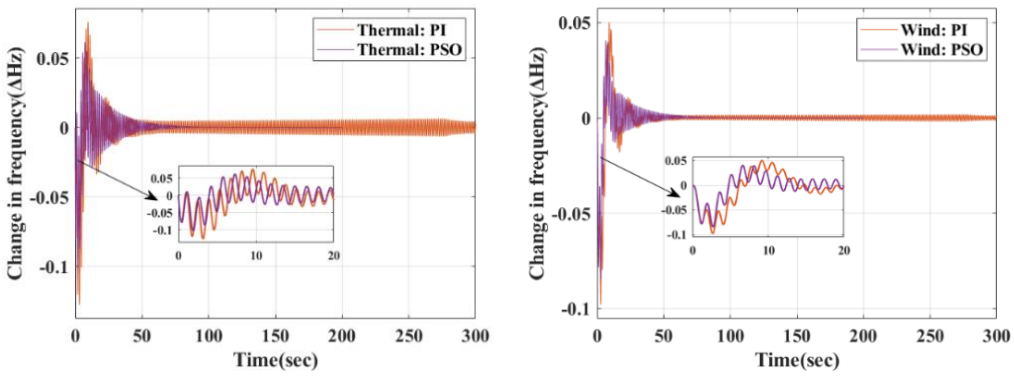

(a) (b)

Fig.10. Evaluation of 5% Change in load in AREA-1; (a) Variations in Area-1 frequency, (b) Variations in Area-2 frequency,

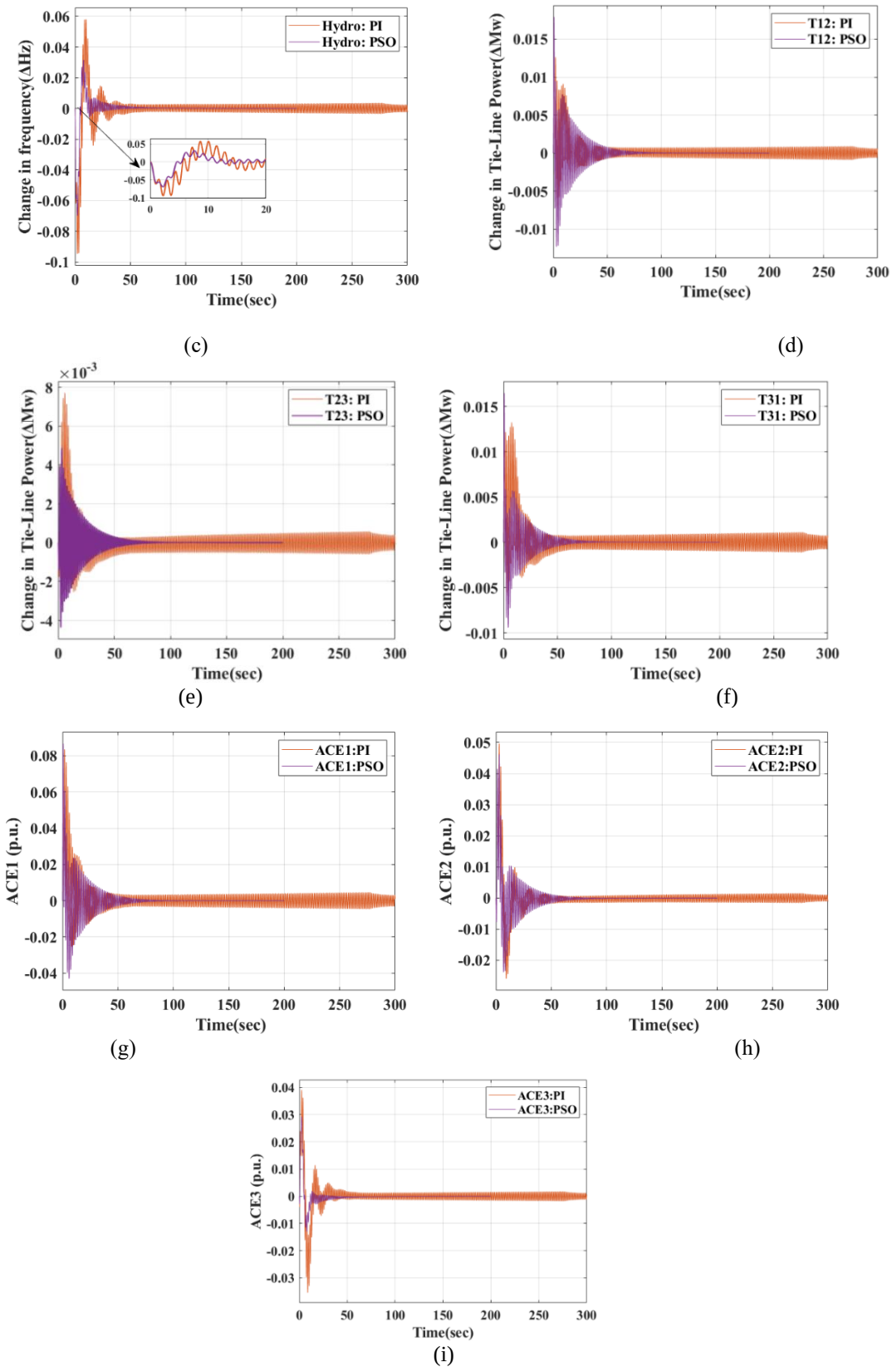

Fig.11. Evaluation of 5% Change in load in AREA-1; (c) Variations in Area-3 frequency, and (d) Variations in Area-1 and Area-2 Tie-Line Power (e) Tie-line power change between Area-2 and Area-3 (f) Tie-line power change between Area-3 and Area-1; Area Control Errors for Areas 1 through 3 are shown in (g), (h), and (i) respectively.

Table:5 Comparison values of Steady State Error, Peak Over Shoot, Peak Under Shoot and Settling Time for 5% Change Load in Area-1

	STEADY STATE ERROR		PEAK OVER SHOOT		PEAK UNDER SHOOT		SETTLING TIME	
	PI	**PSO**	**PI**	**PSO**	**PI**	**PSO**	**PI**	**PSO**
ΔF_1	0.002374	**-0.00001555**	0.07585	**0.06162**	-0.12809	**-0.10405**	oscillate	**90**
ΔF_2	0.000762	**-0.00001369**	0.05022	**0.04080**	-0.097826	**-0.084373**	oscillate	**90**
ΔF_3	-0.002481	**-0.00001436**	0.05800	**0.03160**	-0.094467	**-0.069881**	oscillate	**100**
ΔP_{tie1}	0.002374	**-0.00001555**	**0.01679**	0.01792	**-0.0072912**	-0.012237	oscillate	**120**
ΔP_{tie2}	0.000762	**-0.00001369**	0.007703	**0.004867**	**-0.0038855**	-0.0043717	oscillate	**120**
ΔP_{tie3}	-0.002481	**-0.00001436**	**0.01556**	0.01649	**-0.0059212**	-0.0092496	oscillate	**100**
ACE_1	0.002374	**-0.00001555**	**0.08348**	0.08668	**-0.025303**	-0.042898	oscillate	**100**
ACE_2	0.000762	**-0.00001369**	0.04961	**0.04614**	-0.025971	**-0.023674**	oscillate	**100**
ACE_3	-0.002481	**-0.00001436**	0.03907	**0.02930**	-0.035398	**-0.013054**	oscillate	**120**

IV. CONCLUSION AND FUTURE SCOPE

The design of Load Frequency Control (LFC) for multi-area Thermal-Wind-Hydro power systems is presented in this study. When there is a disruption in the load, control performance is improved by using a proportional integral (PI) controller. The PI Controller's gain settings are optimized by experimenting with the ITSE objective function. In the Reheat thermal area (Area 1), the efficacy of the PI controllers is analyzed and compared for 1%, 2%, and 5% Step Load interruption. The aforementioned system employs an optimized integrated controller for its AGC in the event of an abrupt disruption in load. A comparative study of the performance analysis of various objective functions is conducted using transient response performance measures, such as peak frequency deviation, rising time, steady state error, and settling time. In order to optimize the controller's gains, different objective functions are applied. The study shows that the kind of performance indicator chosen for optimization affects the system's rise and settling times. ITSE objective function-based controllers produce significantly better outcomes (less settling time, peak overshoot and undershoot, dampening oscillations, and steady state error), according to simulation results. Comparisons between PI and PSO-PI controllers are used in order to better optimize the gain values of PI controllers. When compared to the power system response equipped with a standard PI controller, it is shown that the PSO-PI controller efficiently reduces the electromechanical oscillations, settling time, steady state error, peak over, and undershoots. by using several improved algorithms to include additional renewable energy sources into the linked power system problem.

NOMENCLATURE

Three Area System Parameters	
T_g	Time Constant of Governor
T_t	Time Constant of Turbine
T_r	Time Constant of Reheater Thermal Power
T_t	Water Time Constant
K_p	the electric governor proportional gain
U_1	Control outputs from Area-1's controller
U_2	Control Outputs from Area-2's controller
U_3	Control Outputs from the controller of Area-3
A_{12}	Constants for synchronizing coefficients of Tie-Line-1
A_{23}	Constants for synchronizing coefficients of Tie-Line-2

A_{31}	Constants for synchronizing coefficients of Tie-Line-3
ΔP_{tie12}	Incremental shift in tie line power of Tie-Line-1
ΔP_{tie23}	Incremental shift in tie line power of Tie-Line-2
ΔP_{tie31}	Incremental shift in tie line power of Tie-Line-3
T_{12}	Coefficient of synchronization of Tie-Line-1
T_{23}	Coefficient of synchronization of Tie-Line-2
T_{31}	Coefficient of synchronization of Tie-Line-3
Δf_1	Deviations in system frequency in Area-1
Δf_2	Deviations in system frequency in Area-2
Δf_3	Deviations in system frequency in Area-3
K_g	Gain value of Governor
K_t	Gain Value of Turbine
K_r	Coefficient of reheat steam Turbine Constant
K_d	the electric governor derivative gain
K_i	the electric governor integral gains
T_ε	the parasitic time constant
T_{pt}	the main time constant

REFERENCES

[1]. N.E.Y. Kouba, M. Menaa, M. Hasni, M. Boudour, Load Frequency Control in multi-area power system based on Fuzzy Logic-PID Controller, in 2015 IEEE International Conference on Smart Energy Grid Engineering (SEGE), Oshawa, ON, Canada, 2015.

[2]. Dola Gobinda Padhan, Somanath Majhi, "A new control scheme for PID load frequency controller of single-area and multi-area power systems", ISA Transactions, Volume 52, Issue 2,2013, Pages 242-251, ISSN 0019-0578,

[3]. D. H. Tungadio and Y. Sun, "Load frequency controllers considering renewable energy integration in power system," Energy Reports, 2019, vol. 5, pp. 436–453.

[4]. Asma Aziz, Aman Than Oo, Alex Stojcevski," Analysis of frequency sensitive wind plant penetration effect on load frequency control of hybrid power system", International Journal of Electrical Power & Energy Systems, vol.99, pp.603-617, July 2018.

[5]. Sarker, Md, Hasan, Kamrul. "Load Frequency Control in Power System". 10. 23-30. 2016.

[6]. K. Jagatheesan and B. Anand, "Automatic generation control of three area hydro-thermal power systems with electric and mechanical governor," IEEE International Conference on Computational Intelligence and Computing Research, Coimbatore, India, 2014, pp. 1-6.

[7]. Kothari D. P., Nagrath I.J., 2003. Modern Power System Analysis, Tata Mc Gro Hill, Third Edition.

[8]. Prabha S Kundur and Om P Malik. Power system stability and control. McGraw-Hill Education, 2022

[9]. Wadhawa C.L., 2007. "Electric Power System" New Age International Pub. Edition.

[10]. Elgerd O. I. 1971. Electric Energy System Theory; An Introduction, Mc Gro Hill.

[11]. Z. A. Obaid, L. M. Cipcigan, L. Abrahim, and M. T. Muhssin, "Frequency control of future power systems: reviewing and evaluating challenges and new control methods," J. Mod. Power Syst. Clean Energy, 2019, vol. 7, no. 1, pp. 9–25.

[12]. D. K. Gupta, R. Naresh and A. V. Jha, "Automatic Generation Control for Hybrid Hydro-Thermal System using Soft Computing Techniques," 2018 5th IEEE Uttar Pradesh Section International Conference on Electrical, Electronics and Computer Engineering (UPCON), Gorakhpur, 2018, pp. 1-6.

[13]. P. Anil Kumar, J. Shankar "Dynamic Analysis and Stability of the Load Frequency Control in Two Area Power System with Steam Turbine" having ISSN: 2248-9622 Vol. 2, Issue 6, November- December 2012, pp.1573-1577.

[14]. Abdul Latif, S.M. Suhail Hussain, Dulal Chandra Das, Taha Selim Ustun, "State-of-the-art of controllers and soft computing techniques for regulated load frequency management of single/multi-area traditional and renewable energy-based power systems, Applied Energy, Volume 266, 2020, 114858, ISSN 0306-2619

[15]. M. Suman, M. Venu Gopala Rao, G. R. S. Naga Kumar and O. Chandra Sekhar, "Load frequency control of three-unit interconnected multimachine power system with PI and fuzzy controllers," 2014 International Conference on Advances in Electrical Engineering (ICAEE), Vellore, 2014, pp. 1-5.

[16]. Tshinavhe, Ntanganedzeni Ratshitanga, Mukovhe, Tsheme, Nomzamo. Review of Adaptive Load Frequency Control Strategies for Improving Wind Power Plant Integration, 2024, pp 1-6.

[17]. D. H. Tungadio and Y. Sun, "Load frequency controllers considering renewable energy integration in power system," Energy Reports, vol. 5, pp. 436–453, 2019, doi: 10.1016/j.egyr.2019.04.003

[18]. Irfan Ahmed Khan, Hazlie Mukhlis, Nurulafiqah Nadzirah Mansor, Hazlee Azil Illias, Lilik Jamilatul Awalin, Li Wang, "New trends and future directions in load frequency control and flexible power system: A comprehensive review", Alexandria Engineering Journal, Volume 71, 2023, Pages 263-308, ISSN 1110-0168,

[19]. M.H. Soliman, H.E.A. Talaat, M.A. Attia, "Power system frequency control enhancement by optimization of wind energy control system", Ain Shams Eng. J. 12 (4) (Dec. 2021) 3711– 3723, https://doi.org/10.1016/J.ASEJ.2021.03.027

[20]. M. Beus and H. Pandzic, "Application of model predictive control algorithm on a hydro turbine governor control," 20th Power Syst. Comput. Conf. PSCC 2018, pp. 1–7, 2018, doi: 10.23919/PSCC.2018.8442594.

[21]. Ram Babu, N., Bhagat, S.K., Saikia, L.C. et al. A Comprehensive Review of Recent Strategies on Automatic Generation Control/Load Frequency Control in Power Systems. Arch Computat Methods Eng 30, 543–572 (2023). https://doi.org/10.1007/s11831-022-09810-y
[22]. Mohamed M. Ismail, Ahmed F. Bendary, Load Frequency Control for Multi Area Smart Grid based on Advanced Control Techniques, Alexandria Engineering Journal, Volume 57, Issue 4, 2018, Pages 4021-4032, ISSN 1110-0168, https://doi.org/10.1016/j.aej.2018.11.004.
[23]. K. Kaur and Y. Kumar, "Swarm Intelligence and its applications towards Various Computing: A Systematic Review," Proc. Int. Conf. Intell. Eng. Manag. ICIEM 2020, pp. 57–62, 2020, doi: 10.1109/ICIEM48762.2020.9160177.
[24]. S.Prakash, S.K.Sinha, "Simulation based neuro-fuzzy hybrid intelligent PI control approach in fourarea load frequency control of interconnected power system," Int. J. Applied Soft Computing.23, 152–164, 2014.
[25]. M. Osman, M. Elhaj and A. Salem, "Load Frequency Control in Two Area Power System using GA, SA and PSO Algorithms: A Comparative Study," 2021 31st Australasian Universities Power Engineering Conference (AUPEC), Perth, Australia, 2021, pp. 1-8, doi: 10.1109/AUPEC52110.2021.9597705.
[26]. Mohammed Wadi, Abdulfetah Shobole, Wisam Elmasry, Ismail Kucuk,"Load frequency control in smart grids: A review of recent developments,Renewable and Sustainable Energy Reviews", Volume 189, Part A, 2024,114013,ISSN 1364-0321,
[27]. Mohamed M. Ismail, Ahmed F. Bendary, Load Frequency Control for Multi Area Smart Grid based on Advanced Control Techniques, Alexandria Engineering Journal, Volume 57, Issue 4, 2018, Pages 4021-4032, ISSN 1110-0168, https://doi.org/10.1016/j.aej.2018.11.004.
[28]. A Khodabakhshian and R Hooshmand. A new pid controller design for automatic generation control of hydro power systems. International Journal of Electrical Power & Energy Systems, 32(5):375–382, 2010.
[29]. Gayadhar Panda, Sidhartha Panda, and Cemal Ardil. Automatic generation control of interconnected power system with generation rate constraints by hybrid neuro fuzzy approach. International journal of electrical power and energy systems engineering, 2(1):13–18, 2009.
[30]. Xiangjie Liu, Xiaolei Zhan, and Dianwei Qian. Load frequency control considering generation rate constraints. In 2010 8th World Congress on Intelligent Control and Automation, pages 1398–1401. IEEE, 2010.
[31]. Le-Ren Chang-Chien, Wei-Ting Lin, and Yao-Ching Yin. Enhancing frequency response control by dfigs in the high wind penetrated power systems. IEEE transactions on power systems, 26(2):710–718, 2010.
[32]. Naresh Kumari and A N Jha. Particle swarm optimization and gradient descent methods for optimization of pi controller for agc of multiarea thermal-wind-hydro power plants. In 2013 UK Sim 15th International Conference on Computer Modelling and Simulation, pages 536– 541, 2013.
[33]. Prabha S Kundur and Om P Malik. Power system stability and control. McGraw-Hill Education, 2022.
[34]. Nicolaos et.all Munteanu, Iulian. Optimal Control of Wind Energy Systems, Towards a Global Approach. 01 2008.